LAWRENCE
LIVERMORE
NATIONAL
LABORATORY

UCRL-PROC-218719

Long-Term Corrosion Behavior of Alloy 22 in 5 M CaCl2 at 120°C

J. C. Estill, G. A. Hust, K. J. Evans, M. L. Stuart, R. B. Rebak

February 7, 2006

2006 ASME Pressure Vessels and Piping Conference
Vancouver, Canada
July 23, 2006 through July 27, 2006

Proceedings of PVP2006
2006 ASME Pressure Vessels and Piping Division Conference
July 23-27, 2006, Vancouver, British Columbia, Canada
PVP2006-ICPVT11-93422

LONG-TERM CORROSION BEHAVIOR OF ALLOY 22 IN 5 M $CaCl_2$ AT 120°C

John C. Estill **Gary A. Hust**

Kenneth J. Evans **Marshall L. Stuart**

Raúl B. Rebak

Lawrence Livermore National Laboratory
7000 East Ave, L-631
Livermore, California, 94550 USA

ABSTRACT

In conditions where tight crevices exist in hot chloride containing solutions Alloy 22 may suffer crevice corrosion. The occurrence (or not) of crevice corrosion in a given environment (e.g. salt concentration and temperature), is governed by the values of the critical potential (E_{crit}) for crevice corrosion and the corrosion potential (E_{corr}). This paper discusses the evolution of E_{corr} and corrosion rate (CR) of creviced Alloy 22 specimens in 5 M calcium chloride ($CaCl_2$) at 120°C. Tested specimens included non-creviced rods and multiple creviced assemblies (MCA) both non-welded (wrought) and welded. Results show that Alloy 22 suffers crevice corrosion under the open circuit conditions in the aerated hot $CaCl_2$ brine. However, after more than a year immersion the propagation of crevice corrosion was not significant. The general corrosion rate decreased or remained unchanged as the immersion time increased. For rods and MCA specimens, the corrosion rate was lower than 100 nm/year after more than a year immersion time.
Keywords: N06022, Calcium Chloride, Corrosion Potential, Crevice Corrosion

INTRODUCTION

Alloy 22 (N06022) is a nickel base alloy designed to be resistant to all forms of corrosion. Alloy 22 (N06022) contains approximately 56% nickel (Ni), 22% chromium (Cr), 13% molybdenum (Mo), 3% tungsten (W) and 3% iron (Fe) (ASTM B 575). [1] Because of its high level of Cr, Alloy 22 remains passive in most industrial environments and therefore has an exceptionally low general corrosion rate. [2-4] The combined presence of Cr, Mo and W imparts Alloy 22 with high resistance to localized corrosion such as pitting corrosion and stress corrosion cracking even in hot high chloride (Cl-) solutions. [5-10] It has been reported that Alloy 22 may suffer localized corrosion such as crevice corrosion when it is anodically polarized in chloride containing solutions. [6-8,11-13] It is also known that the presence of nitrate (NO_3^-) and other oxyanions in the solution minimizes or eliminates the susceptibility of Alloy 22 to crevice corrosion. [6-8,14-20] The value of the ratio ($[NO_3^-]/([Cl^-]$) has a strong effect of the susceptibility of Alloy 22 to crevice corrosion. [14-22] The higher the nitrate to chloride ratio the stronger the inhibition by nitrate.

From the general and localized corrosion point of view, it is important to know the value of E_{corr} for Alloy 22 under different environmental conditions. [16] The corrosion degradation model for the Yucca Mountain nuclear waste container assumes that localized corrosion will only occur when E_{corr} is equal or greater than a critical potential (E_{crit}). [16] That is, if $E_{corr} < E_{crit}$ or $\Delta E = E_{crit} - E_{corr} > 0$, general or passive corrosion will occur and localized corrosion is not expected. Passive corrosion rates of Alloy 22 are exceptionally low.[7] In environments that promote localized corrosion, E_{crit} is the lowest potential that would initiate crevice corrosion. The value

of E_{crit} is generally ascribed as the repassivation potential for crevice corrosion obtained using the cyclic potentiodynamic polarization (CPP) curve described in ASTM G 61. [16] From the CPP, the repassivation potential is taken as the potential at which the reverse scan line crosses over the forward scan. This potential is called the repassivation potential cross-over (ERCO). By knowing the values of E_{corr} and E_{crit} (ERCO) of Alloy 22, the likelihood or necessary conditions for the alloy to suffer crevice corrosion under natural polarization (e.g. oxygen from air) can be established. Results from similar type of tests for Alloy 22 under different testing conditions can be found elsewhere. [23-25]

The purpose of the current work was to monitor the behavior of E_{corr} and corrosion rate for welded Alloy 22 creviced specimens in 5 M $CaCl_2$ solution at 120°C. The specimens were tested in the mill annealed (MA), in the as-welded (ASW) and also in the as-welded plus high temperature aged (HTA) condition Both rods and creviced specimens were used.

EXPERIMENTAL TECHNIQUE

Alloy 22 (N06022) specimens used to assess corrosion potential (E_{corr}) and corrosion rate (CR) as a function of immersion time were machined from welded 1.25-inch thick plates (~32 mm). Table 1 shows the chemical composition of the heats for the base plate and the welding wire. The plates were welded using the gas tungsten arc welding (GTAW) technique from both sides of the plate using the double V groove technique. The specimens were in the form of multiple crevice assemblies (MCA) (Figure 1) and rods. Both rods and MCA specimens were partially immersed in the electrolyte solutions. The exposed surface area for each type of specimen was different. The 0.25-inch diameter MA rods (Table 1) were immersed 2-inches into the electrolyte and the exposed surface area was 5.4 cm². The ASW and ASW + HTA rods were immersed 0.5-inch deep and the surface area was 2.9 cm². The MCA specimens were immersed 1-inch into the electrolyte and the surface area was 6.2 cm². This surface area did not include the area covered by the crevice formers, which was approximately 1.5 cm². The MCA had a mounting mechanism for the connecting rod explained in ASTM G 5 (Figure 1). [26] Some of the MCA specimens had a weld seam through the center of the cross section. The crevice formers were mounted on both sides of the specimen. Each crevice former consisted of a washer made of a ceramic material containing 12 crevicing spots or teeth with gaps in between the teeth (ASTM G 48). [26] For the welded MCA, the crevice formers rested on a weld and base mix of material. Before mounting them onto the metallic specimens, the CF were covered with PTFE tape to ensure a tight crevicing gap. The specimens had a ground surface finish of 600-grit paper. There were two types of welded MCA specimens in this work (Table 2): (1) The as-welded (ASW) which were as-received welded specimens and (2) the as-welded plus high temperature aged (ASW + HTA). For both welded MCA and welded rods (Table 2), the thermal aging was carried out for 173 hours at 700°C to produce precipitation of second phases such as topologically close packed (TCP) phases. After this high-temperature treatment the specimens were re-polished with 600-grit paper to remove the high-temperature air-formed oxide from the surface.

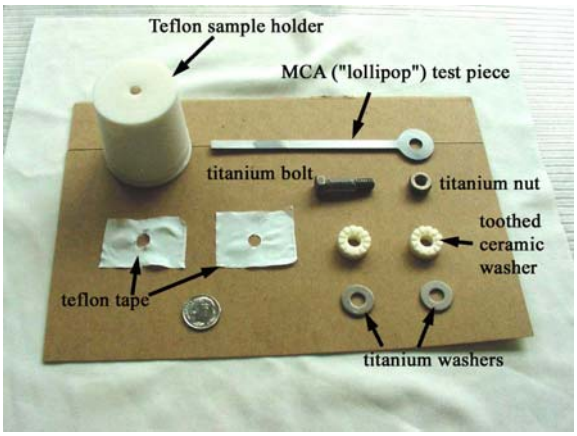

Figure 1. MCA Specimen and hardware

The E_{corr} of a pure platinum rod (ASTM B 561) [1] was also monitored. The platinum rod was 1/8-inch in diameter and 12-inch long. This rod (WEA014 in Table 2) was immersed 1-inch deep into the electrolyte solution.

The testing electrolyte was 5 M (molar) $CaCl_2$ (6.1 *m* or molal) at 120°C. The pH of the solution was approximately 5 to 6. For the cyclic polarization tests the electrolyte was deaerated with purified nitrogen and for the long-term corrosion potential monitoring the electrolyte was naturally aerated (air was circulated above the solution but it was not purged through the solution). The gas stream (N_2 or air) exited the vessel through a condenser to avoid evaporation of the electrolyte. The volume of the electrolyte solution was 2 liters (2 L) for the E_{corr} monitoring and 900 mL for the cyclic polarization tests.

Potentials were monitored using saturated silver chloride electrodes [SSC] through a Luggin capillary. The reference electrode was kept at room temperature using a jacketed electrode holder through which cooled water was re-circulated. The potentials in this paper are reported in the saturated silver chloride scale [SSC]. At ambient temperature, the SSC scale is 199 mV more positive than the normal hydrogen electrode (NHE).

The value of the free corrosion potentials or open circuit potentials were acquired using a commercial data acquisition (DA) unit that had the input resistance set at 10 G-ohm. Typically, the measurements were acquired every minute for the first day and every hour after the first day. The data was logged into in the internal memory of the DA unit and

simultaneously to a spreadsheet in an interfaced personal computer. Usually, data back up was performed monthly.

At the same time that E_{corr} was being monitored for all fourteen (14) Alloy 22 specimens in Cell 20 (Table 2), the polarization resistance (PR) of six specimens was also monitored as a function of time using the ASTM G 59 technique. [26] Polarization resistance measurement was performed in one of different "type" of specimens (e.g. rod vs. MCA) (Table 2). The resistance to polarization was generally measured at monthly intervals. The polarization resistance values ($\Omega.cm^2$) were later converted to corrosion rates (μm/year). To measure the polarization resistance, an initial potential of 20 mV below the corrosion potential (E_{corr}) was ramped to a final potential of 20 mV above E_{corr} at a rate of 0.167 mV/s. Linear fits were constrained to the potential range of 10 mV below E_{corr} to 10 mV above E_{corr}. In plot potential vs. current the slope is defined as Rp or resistance to polarization (ASTM G 59). To calculate Rp, the potential was plotted in the X-axis and the current (dependent variable) in the Y-axis. The Tafel constants, ba and bc, were assumed to be ±0.12 V/decade. Corrosion rates were calculated using Equations 1 and 2

$$i_{corr} = \frac{1}{R_p} \cdot \frac{b_a \cdot b_c}{2.303(b_a + b_c)} \qquad (1)$$

$$CR(\mu m / yr) = k \frac{i_{corr}}{\rho} EW \qquad (2)$$

Where k is a conversion factor (3.27×10^6 $\mu m \cdot g \cdot A^{-1} \cdot cm^{-1} \cdot yr^{-1}$), i_{corr} is the corrosion current density in A/cm², which is calculated from resistance to polarization (Rp) slopes, EW is the equivalent weight of Alloy 22 (23.28), and ρ is the density of Alloy 22 (8.69 g/cm³). The EW was calculated assuming an equivalent dissolution of the major alloying elements as Ni^{2+}, Cr^{3+}, Mo^{6+}, Fe^{2+}, and W^{6+} (ASTM G 102). [26]

The start and finish date for Cell 20 are given in Table 2. Then the specimens were removed from the cells, disassembled and examined under 20X magnification for evidence of localized corrosion (mainly crevice corrosion). Some specimens were studied under a scanning electron microscope.

EXPERIMENTAL RESULTS AND DISCUSSION

Evolution of the Corrosion Potential of Alloy 22

Table 2 lists the E_{corr} for platinum for the fourteen Alloy 22 specimens immersed in Cell 20 at one day after the test started and towards the end of the immersion test (492 days). Table 2 shows that for Alloy 22 the E_{corr} increased as time increased for all the specimens, both rods and MCA. Figure 2 shows the weekly values E_{corr} for Alloy 22 welded rods and platinum. The E_{corr} for ASW rods was approximately steady in time after the first 50 days of immersion and in the order of 0 V (SSC) (see also Table 2). The E_{corr} for the high temperature aged (HTA) welded rod was higher and approximately 200 mV. It is not clear why the E_{corr} of the rod containing TCP phases was higher than for ASW rods.

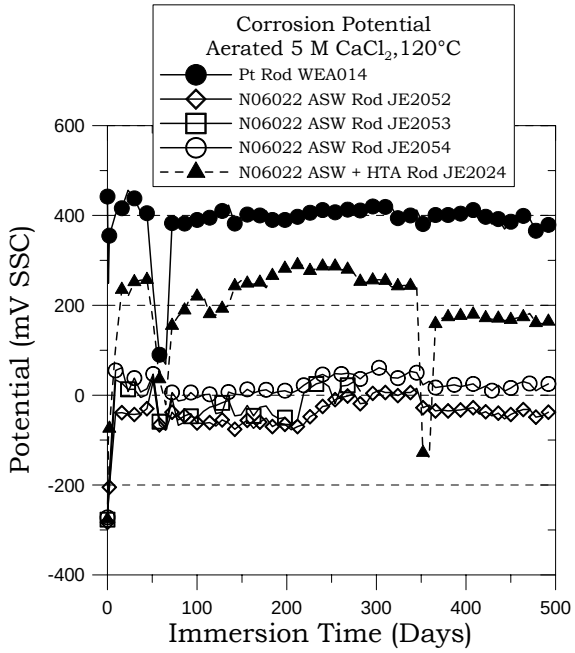

Figure 2. Weekly E_{corr} of Pt and Welded Alloy 22 Rods in aerated 5 M $CaCl_2$ at 120°C

Figure 3 shows the weekly value of E_{corr} as a function of immersion time for the MA (non-welded) Alloy 22 rods. Similarly as in Figure 2, the E_{corr} of the non-welded (MA) rods did not change significantly in time after the first 50 days of immersion. The value of E_{corr} for the non-welded rods was generally between –50 and –150 mV (SSC) (see also Table 2). In general the value of E_{corr} for the welded rods (Fig. 2) was higher than for the non-welded rods (Fig. 3). An explanation cannot be offered at this time for this behavior.

Figures 4 and 5 show respectively the E_{corr} as a function of immersion time of welded and non-welded MCA. Figure 4 also has the data for a welded and HTA MCA specimen. For all the creviced MCA specimens the E_{corr} was practically the same and between –100 and 0 mV (Figures 4-5 and Table 2). That is, the creviced specimens behaved similarly regardless of their metallurgical condition. Figures 2-3 show that for the non-creviced or rod specimens there was an influence of the type of material such as non-welded vs. welded vs. welded plus HTA.

Figure 6 and 7 shows the hourly evolution of E_{corr} vs. time for non-welded Alloy 22 rod and MCA specimens, respectively for the period between immersion days 302 to 323. The fluctuation of the E_{corr} in rods (Fig 6) was more "instantly" nosier than for MCA (Fig 7). However, for the MCA, the longer period fluctuation of the E_{corr} (e.g on a 400 h basis) was approximately twice as large as for the rod specimens (100 mV

vs. 40 mV). The larger fluctuations of E_{corr} for the MCA specimens could be related to the onset and subsequent repassivation of crevice corrosion (Fig. 7).

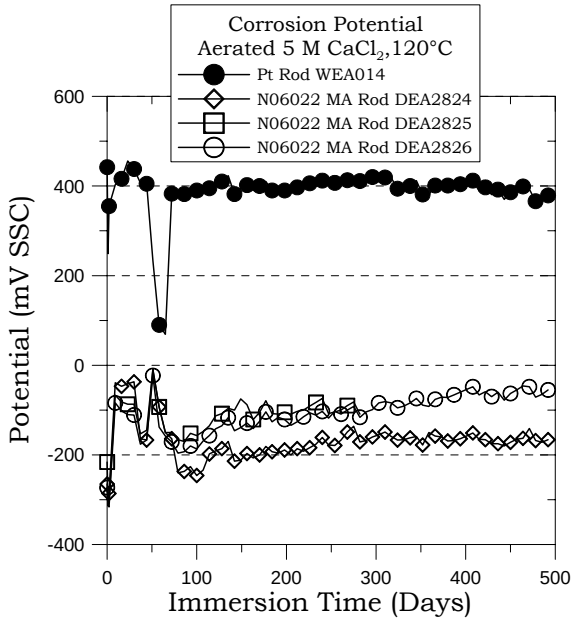

Figure 3. Weekly E_{corr} of Pt and Non-Welded Alloy 22 Rods in aerated 5 M $CaCl_2$ at 120°C

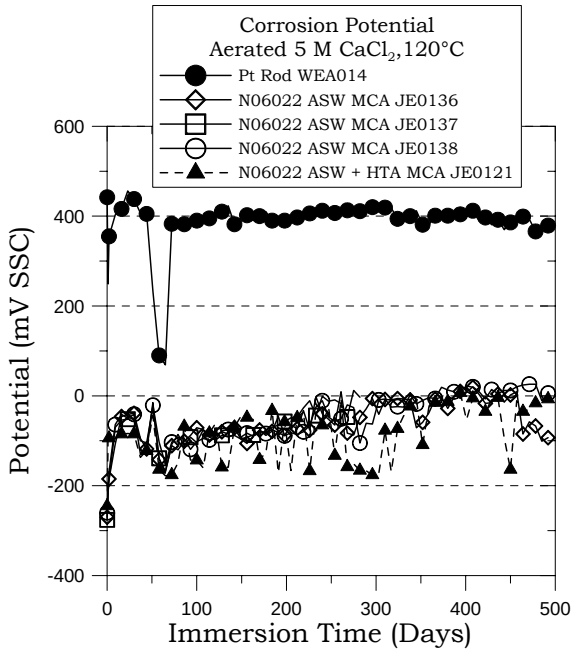

Figure 4. Weekly E_{corr} of Pt and Welded Alloy 22 MCA in aerated 5 M $CaCl_2$ at 120°C

In each cycle (Fig. 7), E_{corr} would increase to near 0 V, initiate crevice corrosion and the E_{corr} would then decrease to near the repassivation potential (see discussions in subsequent sections) of approximately –150 mV, this cathodic direction move would repassivate the specimen and the E_{corr} would thus increase again repeating the cycle.

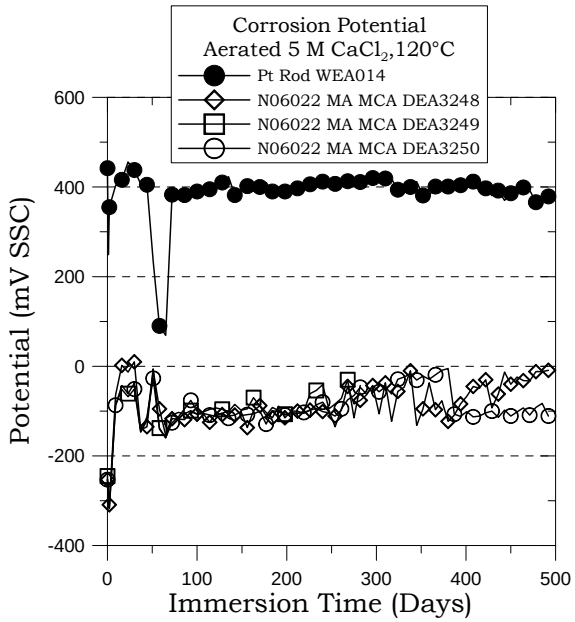

Figure 5. Weekly E_{corr} of Pt and Non-Welded Alloy 22 MCA in aerated 5 M $CaCl_2$ at 120°C

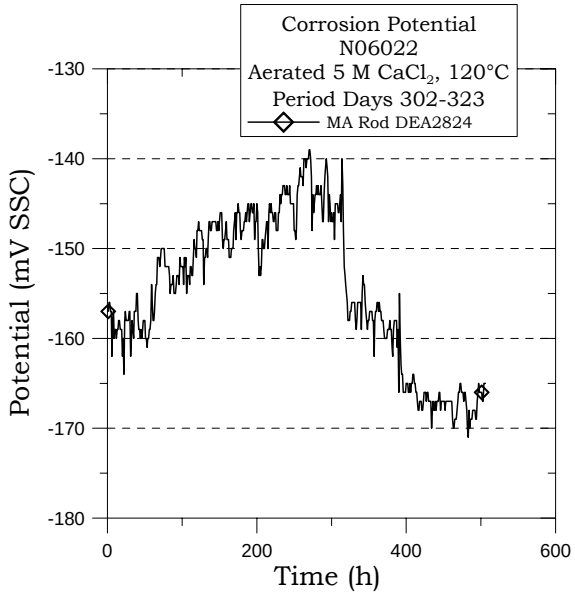

Figure 6. Hourly E_{corr} of Non-Welded Alloy 22 Rod in aerated 5 M $CaCl_2$ at 120°C

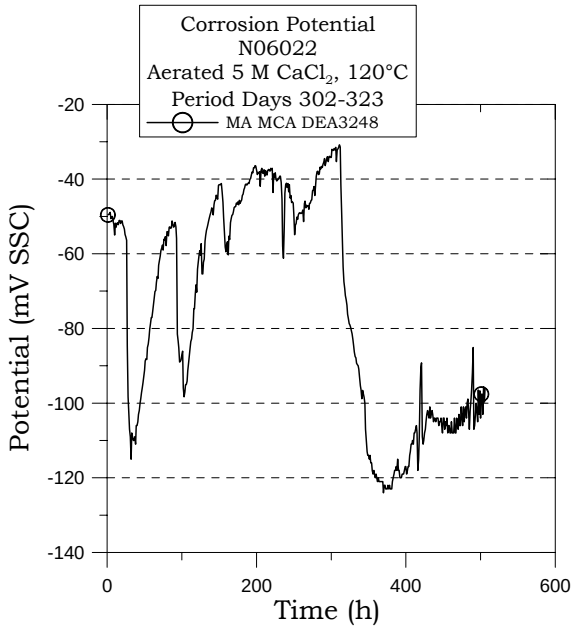

Figure 7. Hourly E_{corr} of Non-Welded Alloy 22 MCA in aerated 5 M $CaCl_2$ at 120°C

Observations of the Specimens After the Tests

The MA (non-welded) rod specimens showed general uneven corrosion. These specimens were manufactured from extruded rods. Even though the testing portion of the rod was polished using 600-grit paper, there were still vestiges of mark in the direction of extrusion of the rod. During the long immersion of near 500 days these marks or dents were preferentially corroded but they cannot be considered to be pitting corrosion. The welded rod specimens were manufactured by machining plates, that is, the surface finish before the start of the test was better (smoother) than for the MA specimens. After the immersion time, only one of the welded rods (JE2052) showed preferential etching of the weld. The other welded rods did not show apparent sign of corrosion. The HTA specimen (JE2024) did not show any preferential attack due to the second phase precipitation in the metal during the thermal treatment. JE2024 was free of any type of visible corrosion in spite of the higher free corrosion potential (Fig. 2)

Both the MA (non-welded) and welded MCA specimens showed crevice corrosion after the long immersion tests of nearly 500 days. Nevertheless the crevice corrosion was mostly circumscribed to only one major site of the crevice former (out of 24 possible sites). Most specimens also had minor attack in two or three other sites. The major crevice corrosion sites were covered by a shiny black oxide film (Figure 8). EDS studies were performed on the oxide and it was found to be rich in Mo and W. All the MCA specimens also showed general corrosion in the non-creviced areas (Figure 9). In some of the specimens there were a tan and bluish tinting suggesting transpassive behavior. The weld seam in the welded MCA was not preferentially attacked compared to the base surrounding metal. The HTA specimen (JE0121) did not show any crevice corrosion and the general corrosion was in the same order of the non-thermally treated specimens. It appears that the specimen may have been attacked from the inside hole but this is not obvious without sectioning the specimen.

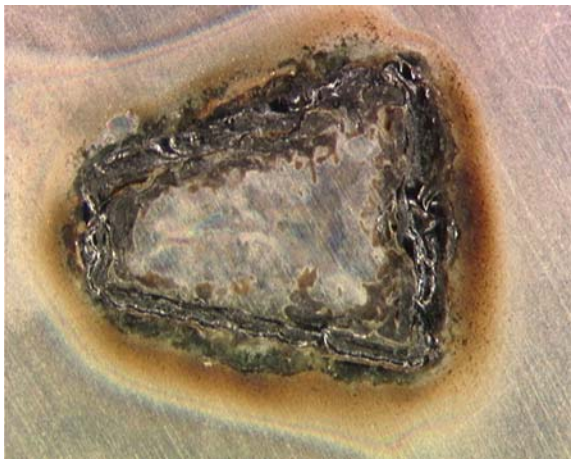

Figure 8. Specimen MA MCA DEA3250. One spot of major crevice corrosion. Magnification X20.

The Repassivation Potential of Alloy 22

In a cyclic potentiodynamic polarization (CPP) curves there are several typical potentials. They can be divided in two groups: (1) Breakdown potentials in the forward scan, called E20 and E200 that represent the potential that needs to be applied to the specimen in the forward scan for the current density to reach respectively 20 μA/cm² and 200 μA/cm².[13,20] The repassivation potentials are called ER10, ER1 and ERCO.[13,20] ER10 and ER1 represent the potentials that need to be applied in the reverse scan for the current density to reach 10 μA/cm² and 1 μA/cm², respectively. ERCO represents the potential at which the reverse scan crosses over (CO) the forward scan in the passive region of potentials. Table 3 shows the repassivation potential for non-welded and welded Alloy 22 in 5 M $CaCl_2$ solution at 120°C. [27] Some of the data in Table 3 has been published before. The average repassivation potential ERCO (cross over) was –188 mV (SSC) for the non-welded specimens and –174 mV (SSC) for the welded specimens. Similarly, the respective ER1 values were –200 and –211 mV, respectively (Table 3). That is, it is expected that if the open circuit potential or free corrosion potential is higher than the values between –233 and –163 mV (considering error bars), crevice corrosion may be initiated in Alloy 22.

Figure 9. Specimen ASW MCA JE0138. One spot of major crevice corrosion and general corrosion in non-crevice areas. Magnification X8.

Figure 10 shows the band of repassivation potentials ER1 and ERCO both for welded and non-welded creviced specimens from CPP (Table 3). Figure 10 also shows the open circuit or corrosion potential for welded and non-welded rods in the same solution. It is clear that the values of E_{corr} were higher than the values of repassivation potential, that is, crevice corrosion should be expected. Observations after the tests (Figs. 8 and 9) show that indeed this was the case. Figs. 8 and 9 also show that even after more than one year immersion the crevice corrosion was not extensive.

The Corrosion Rate of Alloy 22

Figure 11 shows the corrosion rate of Alloy 22 rod specimens as a function of immersion time at 120°C. In general, as the immersion time increased the corrosion rate decreased or remained approximately unchanged. The lowest corrosion rate corresponded to the welded plus HTA specimen correspondingly to its highest corrosion potential (Fig. 2). In general for both the non-welded and welded rods the corrosion rate was only in the order of 100 nm/year.

Figure 12 shows the general corrosion rate of welded and non-welded MCA specimens. In spite that these specimens were undergoing crevice corrosion (DEA3248 and JE0136), their corrosion rate as measured using the polarization resistance test was consistently low and decreasing as the time increased. After one-year immersion the corrosion rate of the creviced coupons was only in the order of 100 nm/year suggesting that the crevice corrosion observed (e.g. Figs 8 and 9) has been stifled or its propagation rate was negligible. The HTA specimen (JE0121) showed slightly higher corrosion rate in spite that this specimen did not suffer crevice corrosion. It appears that this specimen may have suffered some type of localized attack from the inner hole where the oxide film after high temperature treatment may not have been cleaned before immersion. Also Fig. 4 shows that the JE0121 specimen experienced the larger and more frequent fluctuations in potential.

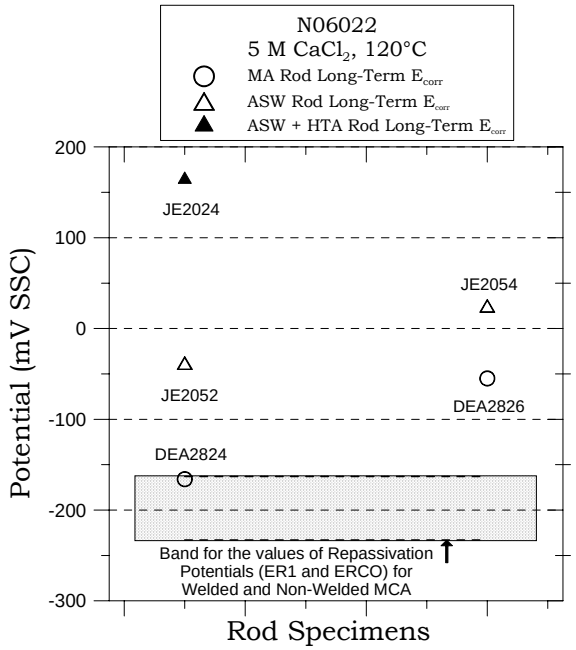

Figure 10. Comparison between E_{corr} (Rods) and Repassivation Potential (MCA).

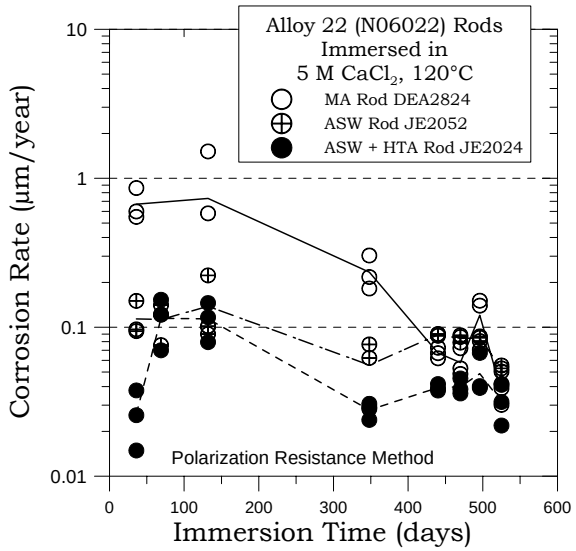

Figure 11. Corrosion Rate as a function of the Immersion time for Alloy 22 rods

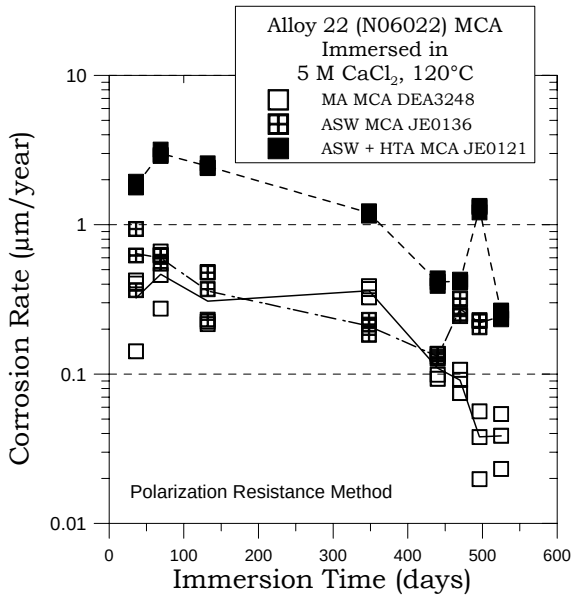

Figure 12. Corrosion Rate as a function of the Immersion time for Alloy 22 MCA

CONCLUSIONS

(1) Results shows that Alloy 22 in highly resistant to both general and localized corrosion in 5 M $CaCl_2$ at 120°C.

(2) Even in the pure chloride brines used here, the general corrosion rate of Alloy 22 was negligible for practical purposes (less than 100 nm/year).

(3) Alloy 22 was prone to crevice corrosion under tight crevices under normal aeration conditions, however the extent of crevice corrosion was not significant.

(4) Crevice corrosion seemed to stifle probably due to the precipitation of corrosion products in or around the creviced area.

(5) The criteria of using the repassivation potential value as a threshold value below which crevice corrosion will not occur seems to be correct.

ACKNOWLEDGMENTS

Sharon G. Torres and her group are acknowledged for performing the high temperature aging the specimens. This work was performed under the auspices of the U. S. Department of Energy by the Uni-versity of California Lawrence Livermore National Laboratory under contract N° W-7405-Eng-48. This work is supported by the Yucca Mountain Project, which is part of the DOE Office of Civilian Radioactive Waste Management (OCRWM)

REFERENCES

1. ASTM International, Volume 02.04, Standard B 575 (ASTM International, 2003: West Conshohocken, PA).
2. Haynes International, "Hastelloy C-22 Alloy", Brochure H-2019E (Haynes International, 1997: Kokomo, IN).
3. R. B. Rebak in Corrosion and Environmental Degradation, Volume II, p. 69, Wiley-VCH, Weinheim, Germany (2000).
4. R. B. Rebak and P. Crook "Influence of the Environment on the General Corrosion Rate of Alloy 22," PVP-Vol 483 pp. 131-136 (ASME, 2004: New York, NY).
5. R. B. Rebak and P. Crook "Improved Pitting and Crevice Corrosion Resistance of Nickel and Cobalt Based Alloys," ECPV 98-17, pp. 289-302 (The Electrochemical Society, 1999: Pennington York, NJ).
6. B. A. Kehler, G. O. Ilevbare and J. R. Scully, Corrosion, 1042 (2001).
7. K. J. Evans and R. B. Rebak in Corrosion Science – A Retrospective and Current Status in Honor of Robert P. Frankenthal, PV 2002-13, p. 344-354 (The Electrochemical Society, 2002: Pennington, NJ).
8. K. J. Evans, S. D. Day, G. O. Ilevbare, M. T. Whalen, K. J. King, G. A. Hust, L. L. Wong, J. C. Estill and R. B. Rebak, PVP-Vol. 467, Transportation, Storage and Disposal of Radioactive Materials – 2003, p. 55 (ASME, 2003: New York, NY).
9. Y-M. Pan, D. S. Dunn and G. A. Cragnolino in Environmentally Assisted Cracking: Predictive Methods for Risk Assessment and Evaluation of Materials, Equipment and Structures, STP 1401, pp. 273-288 (West Conshohocken, PA: ASTM 2000).
10. R. B. Rebak in Environmentally Assisted Cracking: Predictive Methods for Risk Assessment and Evaluation of Materials, Equipment and Structures, STP 1401, pp. 289-300 (West Conshohocken, PA: ASTM 2000).
11. C. S. Brossia, L. Browning, D. S. Dunn, O. C. Moghissi, O. Pensado and L. Yang "Effect of Environment on the Corrosion of Waste Package and Drip Shield Materials," Publication of the Center for Nuclear Waste Regulatory Analyses (CNWRA 2001-03), September 2001.
12. D. S. Dunn, L. Yang, Y.-M. Pan and G. A. Cragnolino "Localized Corrosion Susceptibility of Alloy 22," Paper 03697 (NACE International, 2003: Houston, TX).
13. K. J. Evans, A. Yilmaz, S. D. Day, L. L. Wong, J. C. Estill and R. B. Rebak "Comparison of Electro-chemical Methods to Determine Crevice Corrosion Repassivation Potential of Alloy 22 in Chloride Solutions," JOM, p. 56, January 2005.

14. G. A. Cragnolino, D. S. Dunn and Y.-M. Pan "Localized Corrosion Susceptibility of Alloy 22 as a Waste Package Container Material," Scientific Basis for Nuclear Waste Management XXV, Vol. 713 (Materials Research Society 2002: Warrendale, PA).
15. D. S. Dunn and C. S. Brossia "Assessment of Passive and Localized Corrosion Processes for Alloy 22 as a High-Level Nuclear Waste Container Material," Paper 02548 (NACE International, 2002: Houston, TX).
16. J. H. Lee, T. Summers and R. B. Rebak "A Performance Assessment Model for Localized Corrosion Susceptibility of Alloy 22 in Chloride Containing Brines for High Level Nuclear Waste Disposal Container," Paper 04692 (NACE International, 2004: Houston, TX).
17. G. O. Ilevbare, K. J. King, S. R. Gordon, H. A. Elayat, G. E. Gdowski and T. S. E. Summers, Journal of The Electrochemical Society, 152, 12, B547-B554, 2005
18. D. S. Dunn, L. Yang, C. Wu and G. A. Cragnolino, Material Research Society Symposium, Spring 2004, San Francisco, Proc. Vol 824 (MRS, 2004: Warrendale, PA)
19. D. S. Dunn, Y.-M. Pan, L. Yang and G. A Cragnolino and X. He "Localized Corrosion Resistance and Mechanical Properties of Alloy 22 Waste Package Outer Containers" JOM, January 2005, pp 49-55.
20. R. B. Rebak, Paper 05610, Corrosion/2005 (NACE International, 2005: Houston, TX)
21. D. S. Dunn, Y.-M. Pan, L. Yang and G. A Cragnolino, Corrosion, 61, 11, 1076, 2005
22. G. O. Ilevbare, K. J. King, S. R. Gordon, H. A. Elayat, G. E. Gdowski and T. S. E. Summers, Journal of The Electrochemical Society, 152, 12, B547-B554, 2005
23. J. C. Estill, G. A. Hust and R. B. Rebak "Long Term Corrosion Potential Behavior of Alloy 22," Paper 03688 (NACE International, 2003: Houston, TX).
24. K. J. King, J. C. Estill, G. A. Hust, M. L. Stuart and R. B. Rebak, Paper 05607, Corrosion/2005 (NACE International, 2005: Houston, TX).
25. K. J. Evans, M. L. Stuart, R. A. Etien, G. A. Hust, J. C. Estill and R. B. Rebak, Paper 06623, Corrosion/2006 (NACE International, 2006: Houston, TX).
26. ASTM International, Volume 03.02, Standards G 5, G 48, G 59, G 61, G 102 (ASTM International, 2003: West Conshohocken, PA).
27. G. O. Ilevbare, Unpublished data, Lawrence Livermore National Laboratory, March 2003. .

Table 1. Heats and Approximate Composition of N06022 Specimens

Specimens	Heat - Manufacturer	Approximate Composition
MA Rods DEA2824, DEA2825 and DEA2826	2277-0-3251 Haynes International	~56 Ni, 22 Cr, 14.1 Mo, 2.7 W, 4.5 Fe, 1.3 Co, 0.31 Mn, 0.16 V, 0.03 Si, <0.01 S, 0.01 P, 0.003 C
ASW Rods JE2052, JE2053 and JE2054	Base Plate 059902LL1 by Jessop and Filler Metal Wire XX1753BG (Plate D10) by Inco Alloys International	Base Metal = 59.56 Ni, 20.38 Cr, 13.82 Mo, 2.64 W, 2.85 Fe, 0.01 Co, 0.16 Mn, 0.17 V, 0.05 Si, 0.0002 S, 0.008 P, 0.005 C Filler Metal = 59.7 Ni, 20.54 Cr, 14 Mo, 3.1 W, 2.08 Fe, 0.03 Co, 0.12 Mn, 0.03 V, 0.06 Si, 0.001 S, 0.004 P, 0.004 C
ASW + HTA Rod JE2024		
MA MCA DEA3248, DEA3249 and DEA3250	2277-1-3265 Haynes International	~56 Ni, 21.39 Cr, 13.36 Mo, 2.9 W, 3.77 Fe, 0.81 Co, 0.24 Mn, 0.15 V, 0.02 Si, 0.004 S, 0.009 P, 0.005 C
ASW MCA JE0136, JE0137 and JE0138	Base Plate 059902LL1 and Filler Metal Wire XX1753BG (Plate D1)	See above
ASW + HTA MCA JE0121		
MA MCA DEA3234, DEA3235, DEA3236, DEA3234, DEA3286, DEA3287 and DEA3288	2277-1-3265 Haynes International	See above
ASW MCA JE0034, JE0035 and JE0036	Base Plate 059902LL1 and Filler Metal Wire XX1753BG (Plate D1 and D4)	See above

Table 2. Specimens and Corrosion Potentials for Cell 20

Channel	Specimen Type and Number	E_{corr} (mV, SSC) 1 Day	E_{corr} (mV, SSC) 492 Days
Cell 20: 5 M $CaCl_2$ pH 5.9, 120°C, Starting Date: 11Jun03. Ended Date: 19Nov04. Days in Testing: 527			
		12Jun04	15Oct04
102 - PR	N06022 MA Rod DEA2824	-328	-166
103	N06022 MA Rod DEA2825 [A]	-328	---
104	N06022 MA Rod DEA2826	-326	-55
105 – PR	N06022 ASW Rod JE2052	-290	-38
106	N06022 ASW Rod JE2053 [A]	-291	---
107	N06022 ASW Rod JE2054	-267	25
108 – PR	N06022 ASW + HTA Rod JE2024	-172	164
109 – PR	N06022 MA MCA DEA3248	-339	-9
110	N06022 MA MCA DEA3249 [B]	-325	---
111	N06022 MA MCA DEA3250	-328	-111
112 – PR	N06022 ASW MCA JE0136	-247	-93
113	N06022 ASW MCA JE0137 [B]	-263	---
114	N06022 ASW MCA JE0138	-269	6
115 – PR	N06022 ASW + HTA MCA JE0121	-140	-7
101	Wrought Platinum Rod WEA014	299	379
[A] Specimens Removed on 02Apr04 (296 days) and [B] Specimens removed on 30Apr04 (324 days)			

Table 3. Characteristic Potentials (mV, SSC) from the Cyclic Polarization Curves (CPP)

Specimen ID	Type of Specimen	$E_{corr,}$ 24-h	E20	E200	ER10	ER1	ERCO
DEA3234	MCA, MA	-373	-81	-41	-164	-193	-164
DEA3235	MCA, MA	-288	-10	8	-160	-200	-215
DEA3236	MCA, MA	NA	-44	-19	-166	-185	-177
DEA3234	MCA, MA	-328	-62	-15	-178	-221	-197
DEA3286	MCA, MA	-324	5	---	---	---	---
DEA3287	MCA, MA	-341	-36	---	---	---	---
DEA3288	MCA, MA	-337	-53	---	---	---	---
Ave.± SD		-332 ± 28	-40 ± 30	-17 ± 20	-167 ± 8	-200 ± 15	-188 ± 22
JE0034	MCA, ASW	-365	-64	41	-163	-210	-161
JE0035	MCA, ASW	-353	73	81	-165	-233	-179
JE0036	MCA, ASW	-340	64	80	-156	-190	-182
Ave.± SD		-353 ± 13	24 ± 77	67 ± 23	-161 ± 5	-211 ± 22	-174 ± 11
The CPP test was stopped after the breakdown potential for specimens DEA3286-88.							